Journal of Organometallic Chemistry, 461 (1993) 177–185

JOM 23734

A Mössbauer effect and Fenske–Hall molecular orbital study of some sulfur containing organoiron–cobalt clusters

Margaret L. Buhl and Gary J. Long [1]

Department of Chemistry, University of Missouri-Rolla, MO 65401-0249 (USA)

(Received November 30, 1992; in revised form March 22, 1993)

Abstract

The electronic properties of a series of iron-cobalt clusters, $H_2Fe_3S(CO)_9$ (I), $HFe_2CoS(CO)_9$ (II), $FeCo_2S(CO)_9$ (III), and $Fe_2S_2(CO)_6$ (V) have been studied by the Mössbauer effect at 78K. The electronic properties of these clusters and $Co_3(CO)_9S$ (IV) have also been studied theoretically with Fenske–Hall molecular orbital calculations. The Mössbauer effect isomer shifts in clusters I–III and V are small and positive, ranging from 0.00 to 0.076 mm/s. The quadrupole splittings range from 0.563 to 1.109 mm/s. The s-electron density, measured by the Mössbauer effect, is similar for clusters with two iron-hydrogen groups or one iron-hydrogen group and one cobalt atom. The s-electron density is also similar for clusters with two iron-hydrogen groups or two cobalt atoms. The quadrupole splittings show a general increase with a decrease in the hydrogen content and an increase in the cobalt content. The cobalt carbonyl ligand charges and the cobalt charges are nearly constant. The sum of the iron and hydrogen charges increases as the iron carbonyl ligand charge decreases. The iron electronic configuration which begins with the $4s^03d^84p^0$ atomic configuration, becomes on average, $4s^{0.35}3d^{6.80}4p^{0.83}$ with a range from $4s^{0.34}3d^{6.80}4p^{0.74}$ in I to $4s^{0.31}3d^{6.85}4p^{0.89}$ in V. The cobalt electronic configuration which begins with the $4s^03d^94p^0$ atomic configuration, becomes on average, $4s^{0.43}3d^{7.67}4p^{1.13}$ with a range from $4s^{0.41}3d^{7.70}4p^{1.08}$ in IV to $4s^{0.44}3d^{7.66}4p^{1.17}$ in II. The isomer shift is well correlated with the sum of the iron 4s Mulliken population and the Clementi and Raimondi effective nuclear charge which they experience. The Mulliken charges and the coefficients of the molecular wave functions are used to calculate the quadrupole splittings in I–III and V.

1. Introduction

The importance of organometallic clusters as models of metal surfaces during the processes of chemisorption and catalysis is well known [1]. Metal-sulfur clusters are particularly important as models of the metal surface during the process of hydrodesulfurization [2–4] in which the sulfur in petroleum or coal is removed by hydrogenating the sulfur-containing compounds to produce hydrogen sulfide and desulfurized organic compounds [5–10]. One catalyst used for hydrodesulfurization is made of cobalt and molybdenum oxides on an alumina support. The rough metal surfaces of the catalyst are often presulfurized, a process which both permits improved catalytic selectivity by preferentially blocking reactions that need multiple catalytic surface sites, and stabilizes the long term activity of the catalyst [5–10]. The presulfurized catalyst corresponds to Co_9S_8/MoS_2. Thus, organometallic clusters can also serve as models of the sulfur poisoning of catalysts [2–4].

Some of the more fundamental interest in $Co_3(CO)_9S$ and $FeCo_2(CO)_9S$ concerns differences in the effects of the unpaired electron on the structure of $Co_3(CO)_9S$ as compared with $FeCo_2(CO)_9S$, which has no unpaired electron [11–13]. Stevenson *et al.* [11] found that, although the single bond covalent radii of cobalt and iron were similar, the average metal–metal bond lengths in $FeCo_2(CO)_9S$ were found to be 0.083 Å shorter than in $Co_3(CO)_9S$. It has been suggested [11,12] that this decrease is a result of the unpaired electron in $Co_3(CO)_9S$ which occupies a molecular orbital that is antibonding with respect to the cobalt atomic orbitals, an occupancy which would yield a weaker and thus longer cobalt–cobalt bond.

Previous Fenske–Hall molecular orbital calculations by Chesky and Hall [2,3] on $H_2Fe_3S(CO)_9$ (I), $HFe_2CoS(CO)_9$ (II), $FeCo_2S(CO)_9$ (III), and $Co_3S(CO)_9$ (IV)

Correspondence to: Dr. G.J. Long.

[1] Address until August 1994: Institut de Physique, Université de Liège, B-4000 Sant-Tilman, Belgium.

0022-328X/93/$6.00

were performed by using a fragment technique in which the clusters were formed from three metal tricarbonyl fragments, a capping sulfur atom, and the appropriate hydrogen atoms. The HOMO of a $Co(CO)_3$ fragment, which has one unpaired electron, was composed primarily of cobalt 3d and 4p atomic orbitals. In contrast, the LUMO of a $Co(CO)_3$ fragment was composed primarily of cobalt 4p and 4s atomic orbitals. The atomic orbitals making up the $Fe(CO)_3$ fragment were similar but higher in energy than those of the $Co(CO)_3$ fragment. The lower energy $Co(CO)_3$ fragment orbitals consist of combinations of the carbon and oxygen atomic orbitals. "Despite" the fact that lower energy fragment orbitals may be delocalized over the entire cluster, they do not contribute to cluster formation" [3]. Upon formation of $Co_3(CO)_9S$, the higher energy $Co(CO)_3$ fragment orbitals combined with the sulfur 3p atomic orbitals. The HOMO of $Co_3(CO)_9S$ had cobalt–cobalt antibonding character and the cobalt–cobalt bonding actually occurred at energies below the HOMO. The formation of $FeCo_2(CO)_9S$ from fragment orbitals was similar to the formation of $Co_3(CO)_9S$, but, in contrast, the HOMO of $FeCo_2(CO)_9S$ has metal–metal bonding character. In both clusters the sulfur 3p atomic orbital gained electron density, as revealed by the -0.13 and -0.17 charge of the sulfur atom in $Co_3(CO)_9S$ and $FeCo_2(CO)_9S$, respectively. Upon formation of $HFe_2CoS(CO)_9$ and $H_2Fe_3S(CO)_9$, both the sulfur and hydrogen atoms also gain electron density. Hence, the charges on the sulfur and hydrogen atoms are -0.25 and -0.14, respectively, in $HFe_2CoS(CO)_9$ and -0.16 and -0.14, respectively, in $H_2Fe_3S(CO)_9$.

The perturbation of the metal-sulfur framework by the nine carbonyl ligands was also considered by Chesky and Hall [3]. The bonding of the nine carbonyl ligands to the metal-sulfur framework resulted in a reduction in the metal–metal bonding. The carbonyl 2π orbitals were found to stabilize the metal–metal antibonding orbitals by accepting electron density. When comparing the results of the molecular orbital calculations of the iron-cobalt clusters, it was noted [3] that the HOMO–LUMO gap increased as the iron and hydrogen content of the cluster increased. This occurred because the number of metal–hydrogen–metal molecular orbitals increased, whereas the number of high energy metal–metal bonding molecular orbitals decreased, thereby increasing the HOMO–LUMO gap.

In this work the electronic properties of the iron-cobalt clusters, $H_2Fe_3S(CO)_9$ **(I)**, $HFe_2CoS(CO)_9$ **(II)**, $FeCo_2S(CO)_9$ **(III)**, and $Fe_2S_2(CO)_6$ **(V)** have been investigated by studying their Mössbauer effect hyperfine parameters, and the results of Fenske–Hall molecular orbital calculations on these clusters and

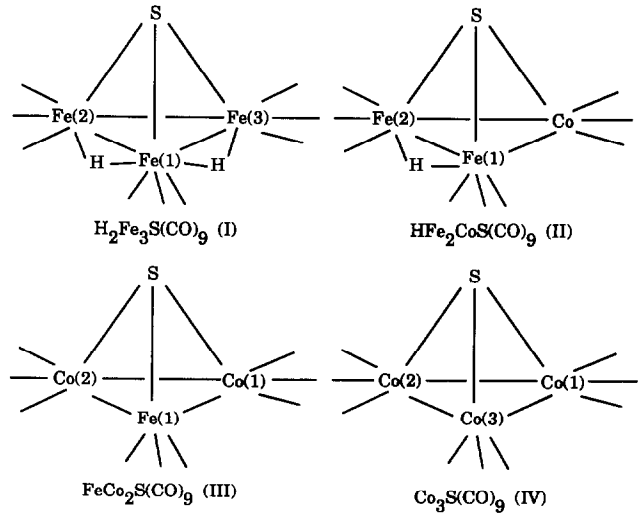

Fig. 1. The structures and numbering schemes for the clusters.

$Co_3(CO)_9S$ **(IV)**. The structures of the clusters are shown schematically in Fig. 1. The molecular orbital calculations aid in the interpretation of the Mössbauer spectra and are used to calculate both the effective nuclear charge experienced by the iron nucleus for comparison with the observed isomer shift, and the electric field gradient at the iron sites, for comparison with the observed quadrupole splitting.

2. Experimental section

The iron-cobalt clusters were prepared according to standard literature methods [14–16]. The aqueous solutions and the organic solvents were degassed prior to use by bubbling nitrogen through them. The hexane used as a solvent in the preparation of $FeCo_2S(CO)_9$ **(III)** was also vacuum distilled under nitrogen to remove the dissolved oxygen. The $Fe_2(CO)_6S_2$ **(V)**, required to prepare $FeCo_2S(CO)_9$ **(III)**, was prepared according to the method of Bogan *et al.* [17] except that the solution was acidified with 100 ml of 6 M HCl instead of 200 ml of 3 M HCl.

The Mössbauer spectra were measured at 78 K on a conventional constant acceleration spectrometer which utilized a room temperature rhodium matrix cobalt-57 source and was calibrated at room temperature with natural abundance α-iron foil. The spectra were fit to symmetric Lorentzian doublets with equal line widths by using standard least-squares computer minimization techniques. The error limit on the isomer shift is ± 0.005 mm/s, ± 0.01 mm/s on the quadrupole splittings and the line widths, and at most ± 1 percent for the relative areas.

The molecular orbital calculations were performed by using the FENSKE-HALL method [1,18,19]. The atomic

basis functions used were those of Herman and Skillman [20] as modified with the $X\alpha$ to Slater basis program of Bursten and Fenske [21–24]. All of the Fenske–Hall calculations used the same basis functions and no effort was made to investigate the influence of changes in these functions on the calculated Mössbauer spectral parameters. The typical error limit for the absolute metal charges obtained from the Fenske–Hall molecular orbital calculations is estimated to be ± 0.06. The typical error limits for the absolute sulfur, hydrogen, and carbonyl ligand charges, and for the atomic orbital populations are estimated to be ± 0.15 or better. The relative error for a series of compounds is probably a factor of two or three smaller. The atomic positions required for the Fenske–Hall molecular orbital calculations of the iron-cobalt clusters were taken from the known X-ray structure of $FeCo_2(CO)_9S$ **(III)** [11]. The hydrogens [3] in $H_2Fe_3S(CO)_9$ **(I)** and $HFe_2CoS(CO)_9$ **(II)** were placed in the metal–sulfur–metal plane below the metal–metal–metal plane at an iron to hydrogen symmetric bridging bond length [25] of 1.879 Å.

The Mulliken charges and the molecular orbital wave functions, obtained from the Fenske–Hall molecular orbital calculations, were used to calculate [1] the electric field gradient at the metal site. The $\langle r^{-3}\rangle_{3d}$ and $\langle r^{-3}\rangle_{4p}$ expectation values for iron were calculated from the 3d Mulliken orbital populations, whereas those for the other metal were held at the constant values of 32.0 for $\langle r^{-3}\rangle_{3d}$ and 11.6 for $\langle r^{-3}\rangle_{4p}$ [26–28].

3. Results and discussion

3.1. Mössbauer effect spectra

The Mössbauer effect spectra of the iron-cobalt clusters studied in this work are shown in Fig. 2, and the derived spectral hyperfine parameters are given in Table 1. Figure 1 shows that the structure of $H_2Fe_3S(CO)_9$ **(I)** has two different types of iron sites, Fe(1) and the chemically equivalent Fe(2) and Fe(3) sites. As a result the Mössbauer spectrum of this cluster was fit with two symmetric quadrupole doublets with an area ratio of approximately one to two, with the small area doublet assigned to Fe(1). As shown in Fig. 1, both of the iron sites in $HFe_2CoS(CO)_9$ **(II)** and in $Fe_2S_2(CO)_6$ **(V)** are chemically equivalent and the Mössbauer spectrum of these clusters were successfully fit with one symmetric quadrupole doublet as was the Mössbauer spectrum of $FeCo_2S(CO)_9$ **(III)**.

The Mössbauer effect spectra of $H_2Fe_3S(CO)_9$ **(I)** and $HFe_2CoS(CO)_9$ **(II)** have been previously measured by Markó, *et al.* [14,15,29*]. For some unknown

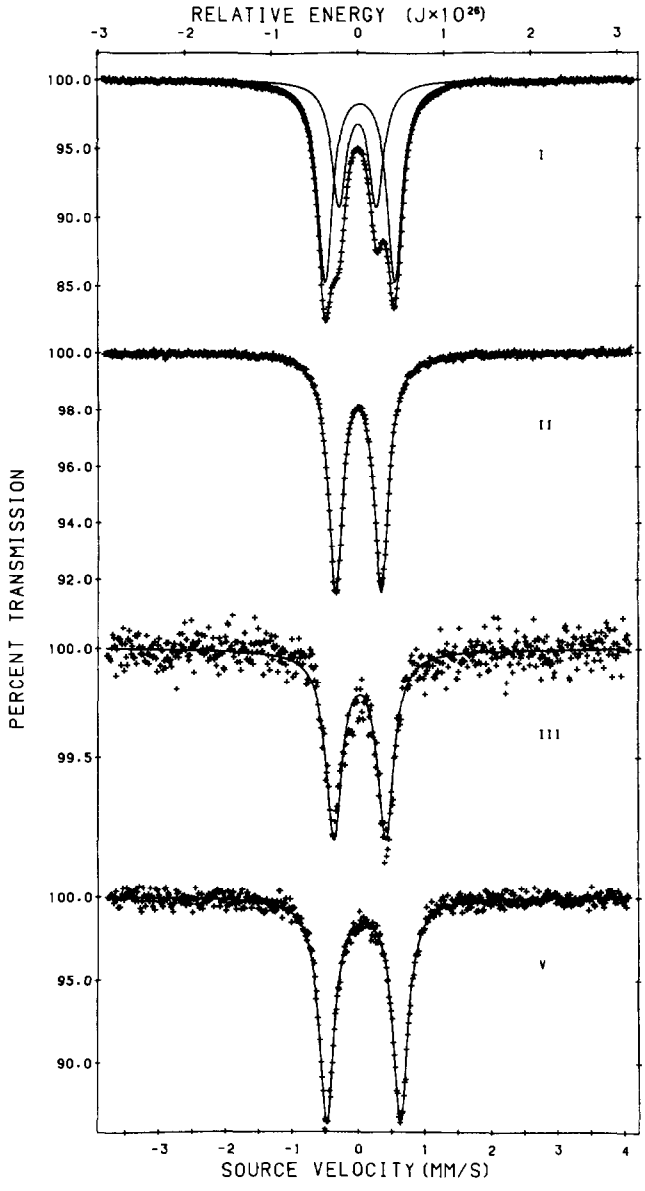

Fig. 2. The Mössbauer effect spectra of clusters I–III and V obtained at 78 K.

TABLE 1. Mössbauer effect spectral parameters [a]

Cluster	Site	δ	ΔE_Q	Γ	% Area
$H_2Fe_3S(CO)_9$ (I)	Fe(1)	0.000	0.563	0.27	37.7
	Fe(2,3)	0.032	1.046	0.27	62.3
$HFe_2CoS(CO)_9$ (II)	Fe(1,2)	0.009	0.689	0.26	100.0
$FeCo_2S(CO)_9$ (III)	Fe(1)	0.023	0.780	0.29	100.0
$Fe_2S_2(CO)_6$ (V)	Fe(1,2)	0.076	1.109	0.27	100.0

[a] All data measured at 78 K and reported relative to room temperature natural abundance α-iron foil. The values are measured in mm/s.

* Reference number with an asterisk indicates a note in the list of references.

TABLE 2. Fenske–Hall molecular orbital results

Cluster	Site	Mulliken atomic orbital population			Charge				HOMO–LUMO Gap	Z_{eff} [a]	Z_{eff} [b]
		3d	4s	4p	Metal	Avg CO	S	H			
$H_2Fe_3S(CO)_9$ (I)	Fe(1)	6.80	0.34	0.74	0.13	0.04	−0.21	−0.09	3.86	3.17	4.71
	Fe(2)	6.80	0.36	0.83	0.01	0.03				3.13	4.70
	Fe(3)	6.78	0.36	0.84	0.02	0.01				3.14	4.72
$HFe_2CoS(CO)_9$ (II)	Fe(1)	6.77	0.36	0.80	0.06	0.01	−0.14	−0.10	3.49	3.16	4.73
	Fe(2)	6.78	0.36	0.80	0.06	0.04				3.15	4.72
	Co	7.66	0.44	1.17	−0.27	0.08				3.28	4.95
$FeCo_2S(CO)_9$ (III)	Fe	6.74	0.39	0.87	0.00	−0.01	−0.08	–	2.75	3.16	4.75
	Co(1)	7.65	0.43	1.14	−0.22	0.09				3.30	4.97
	Co(2)	7.67	0.43	1.12	−0.22	0.10				3.29	4.95
$Co_3S(CO)_9$ (IV)	Co(1)	7.65	0.43	1.14	−0.22	0.03	−0.05	–	1.95	3.30	4.97
	Co(2)	7.70	0.41	1.08	−0.19	0.11				3.27	4.93
	Co(3)	7.70	0.41	1.11	−0.23	0.09				3.26	4.92
$Fe_2S_2(CO)_6$ (V)	Fe(1)	6.85	0.31	0.89	−0.04	0.00	0.01	–	4.77	3.07	4.66
	Fe(2)	6.87	0.30	0.86	−0.04	0.02	0.00	–		3.06	4.64

[a] Effective nuclear charge, experienced by the metal 4s electrons, calculated by using the method of Slater [38,39] and the Mulliken atomic populations. [b] Effective nuclear charge, experienced by the metal 4s electrons, calculated by using the method of Clementi and Raimondi [38] and the Mulliken atomic populations.

reason, the hyperfine parameters we observe do not agree well with those reported [14,15] However, in general the trends in the two sets of parameters are similar.

3.2. Fenske–Hall molecular orbital calculations

In clusters **I–III**, as the iron and hydrogen atoms are replaced with a cobalt, the number of valence electrons remains constant at forty, whereas in cluster **IV** there are forty-one valence electrons. The differences and similarities in the electronic properties of these clusters may be better understood by an investigation of the atomic charges and the overlap populations obtained from the molecular orbital calculations. These differences and similarities are also considered in terms of the iron and cobalt Allred–Rochow electronegativities, 1.64 and 1.70, respectively [30]. The atomic charges of the clusters are given in Table 2. The average carbonyl ligand, carbon, and oxygen charges are shown in Fig. 3, and the sulfur and the average metal charges are shown in Fig. 4.

The similar hydrogen charges in clusters **I** and **II** result from the similarities in the hydrogen coordination environment. In contrast to anionic clusters [31], these neutral clusters show, as expected, little, if any, metal electron delocalization onto their virtually neutral carbonyl ligands. Carbonyl ligands act as Lewis bases by donating electron density to the cobalt and iron atoms. Cobalt is more electronegative than iron and will attract more electron density from the carbonyl ligands than will iron. The average cobalt carbonyl ligand charge (Fig. 3) is thus more positive than the average iron carbonyl ligand charge. Although the average cobalt carbonyl ligand charges in these clusters are constant, the average cobalt carbonyl carbon

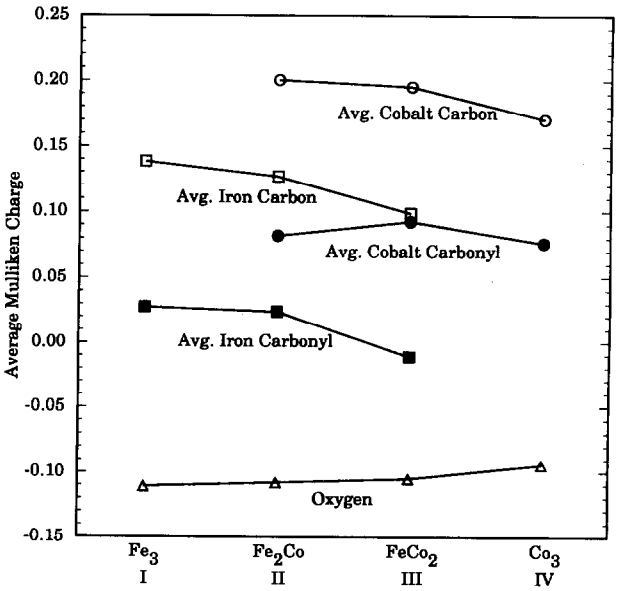

Fig. 3. The average cobalt carbonyl ligand (●), the cobalt carbonyl carbon (○), the iron carbonyl ligand (■), the iron carbonyl carbon (□), and the carbonyl oxygen (△) charges. In this and other figures the iron-cobalt cluster is indicated at the bottom of the figure.

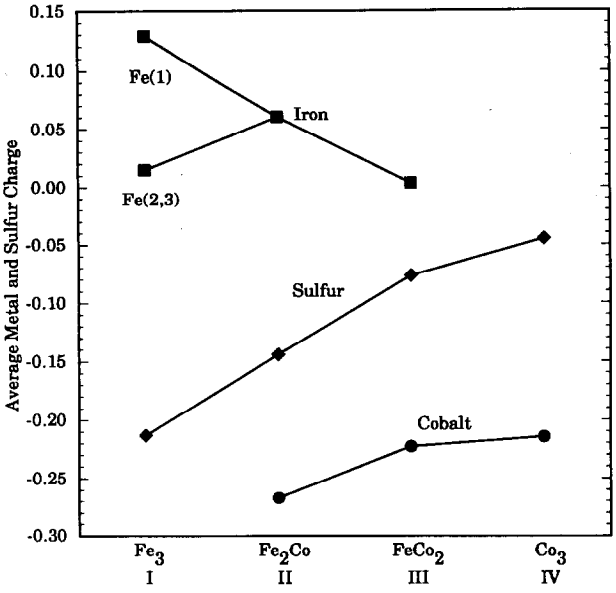

Fig. 4. The average iron (■), the cobalt (●), and the sulfur (◆) charges.

charges decrease slightly in going from clusters **II** to **IV**. This indicates that the donation of electron density to the cobalt atom decreases slightly as may be seen in the slight increase in the cobalt charge.

The average iron carbonyl ligand charge shows a slight decrease in going from clusters **I** to **III**, which indicates that the iron carbonyl carbon is donating more electron density to the iron atoms. However, the iron charge does not show the expected increase in going from clusters **I** to **III**. The electron density accepted by the iron atoms in clusters **I** and **II** is delocalized onto the hydrogen atoms. If the hydrogen charge is added to the iron charge, the resulting charge, increases as the iron carbonyl carbon charge decreases.

The other Lewis base in these clusters is the sulfide ligand. As shown in Fig. 4, the sulfide charge increases as the cobalt content in the clusters increases. The electronegativity of cobalt is greater than that of iron, and as the cobalt content in the clusters increases, the total cluster metal electronegativity increases, the sulfide ligand donates more electron density to the metals, and the sulfide charge increases. The correlation between the decreasing iron charge and the increasing sulfide charge, in going from cluster **I** to **III**, is misleading. The 0.39 average metal–sulfide overlap population is considerably less than the 0.78 average metal–carbon overlap population because the metal–sulfide bond length is greater than the metal–carbon bond length. Further, the sulfide–metal overlap population is typically fifteen percent of the total metal overlap population. Therefore the impact of the sulfide donated electron density upon the metal charges is small compared with that of the carbonyl carbon.

The metal coordination environment influences the metal charge. In cluster **I**, the chemically unique Fe(1) donates electron density to two hydrogen atoms, whereas the chemically equivalent Fe(2,3) each donate electron density to only one hydrogen atom. Hence the Fe(1) charge in cluster **I** is greater than that of Fe(2,3). As the cobalt content in the iron-cobalt clusters increases, the average iron charge decreases from 0.13 to 0.00. In an iron–cobalt bond, more electron density is drawn toward the cobalt atom resulting in a more positive iron charge.

Carbonyl ligands are thought to serve as models of chemisorbed carbon monoxide on a metal surface [32,33]. It is also proposed that the electronic properties of a terminal carbonyl ligand are relatively unchanged from those in carbon monoxide [34]. A comparison of the carbon monoxide and the carbonyl ligand carbon and oxygen charges and overlap populations is a test of this proposal. A carbon monoxide molecule, which has a bond length of 1.128 Å, has a carbon charge of −0.095, and oxygen charge of 0.095, and an overlap population of 1.57. A carbon monoxide molecule which has a bond length of 1.16 Å, the average carbon–oxygen distance of the carbonyl ligands in these clusters, was found to have a carbon charge of −0.068, an oxygen charge of 0.068, and an overlap population of 1.55. In these iron–cobalt clusters, the average carbonyl ligand carbon charge is 0.16, the average oxygen charge is −0.11, and the average carbon–oxygen overlap population is 1.52. The negative carbon monoxide carbon charge enables it to serve as a Lewis base. A more detailed look at the carbon–oxygen overlap populations of both carbon monoxide and the carbonyl ligand is presented in Table 3. The carbon monoxide and carbonyl ligand carbon 2s to oxygen 2s overlap populations are similar, as are those

TABLE 3. A comparison of the CO and carbonyl ligand overlap populations

Species	CO bond length, Å	Oxygen orbital	C, 2s	C, 2p	C, total
CO	1.128	O, 2s	0.21	0.18	0.39
		O, 2p	0.03	1.15	1.18
		O, total	0.24	1.33	1.57
CO	1.16 [a]	O, 2s	0.20	0.18	0.38
		O, 2p	0.04	1.13	1.17
		O, total	0.24	1.31	1.55
Carbonyl ligand [a]	1.16	O, 2s	0.16	0.23	0.39
		O, 2p	0.25	0.88	1.13
		O, total	0.41	1.11	1.52

[a] The average of the thirty-six terminal carbonyl ligands in clusters **I–IV**.

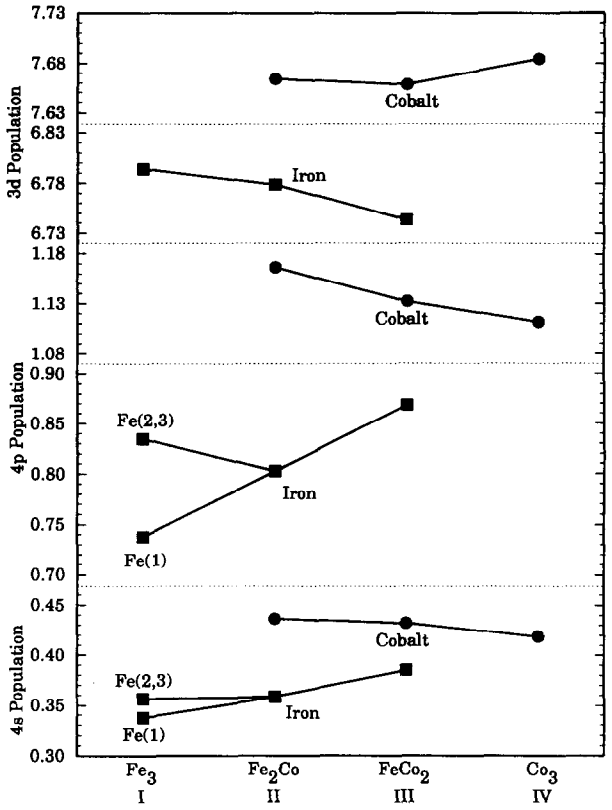

Fig. 5. The average of the iron (■), and the cobalt (●) Mulliken atomic orbital populations.

of carbon 2p to oxygen 2s. The carbonyl carbon 2p to metal overlap population is twice that of the carbonyl carbon 2s to metal overlap population. As the carbonyl carbon donates electron density to the metal, the carbonyl carbon 2p to oxygen 2p overlap population decreases as compared to that of carbon monoxide. The increase in the carbonyl carbon 2s to oxygen 2p overlap population, as compared to that of carbon monoxide, may be due to the delocalization of the metal electron density which the carbonyl carbon 2p orbital accepts because of metal π-back bonding. Overall the carbonyl ligand carbon–oxygen overlap population is similar to that of carbon monoxide, and thus their overall electronic properties are similar. Also the small differences in the specific carbon–oxygen orbital overlap populations make carbonyl ligands satisfactory models for chemisorbed carbon monoxide on a metal surface.

Figure 5 shows the metal Mulliken atomic orbital populations of these clusters. The iron 4s and 3d populations are constant, as are the iron 4s and 3d to near-neighbor overlap populations. The greatest range in the atomic orbital populations occurs in the iron 4p atomic orbitals. In cluster **I**, the 0.52 Fe(1) 4p to near-neighbor overlap population is less than the 0.63 Fe(2,3) 4p to near-neighbor overlap population, which leads to a lesser Fe(1) 4p orbital population. The iron 4p to near-neighbor overlap population increases to 0.76 in cluster **III**, which also leads to an increase in the iron orbital population. The cobalt 4s, 4p, and 3d populations are constant, as are the cobalt to near-neighbor overlap populations. A comparison of the orbital populations of the forty valence electron cluster **III** and the forty-one valence electron cluster **IV**, shows that the extra electron in cluster **IV** is localized predominately in the Co(3) 3d orbital. This is the cobalt atom in cluster **IV** which replaced the iron atom in cluster **III**. This is seen in Fig. 5 as a slight increase in the cobalt 3d orbital population in going from cluster **III** to **IV**.

Although the results given in Table 2 are noticeably different from the results obtained by Chesky and Hall [3,35 *], most of the trends are the same. Chesky and Hall [3] found that the unique Fe(1) charge in **I** is more positive than that of the equivalent irons, Fe(2,3). In agreement with our results, they also found [3] that the iron charges in **II** and **III** were more positive than those of cobalt. We also find that the hydrogen charge in clusters **I** and **II** was constant and negative. Chesky and Hall [3] found that the sulfur charge was more positive than that of cobalt, whereas we find just the opposite [35]. Our calculations [1] reveal that the HOMO–LUMO gap increases almost linearly with the iron content of the cluster with a slope of 0.65 eV per iron, an intercept of 2.04 eV and a correlation coefficient of 0.99. As mentioned above, Chesky and Hall [3] also saw this trend and attributed it to the decrease in the number of high energy metal–metal bonding molecular orbitals.

3.3. Mössbauer effect isomer shift

The results of the Fenske–Hall molecular orbital calculations, given in Table 2, may be used to understand the variations in the Mössbauer effect isomer shifts. As the s-electron density at the iron nucleus decreases, the isomer shift increases. The s-electron density at the iron nucleus can be represented by the iron 4s Mulliken atomic population obtained from the molecular orbital calculations. Therefore it is expected that, as the iron 4s Mulliken atomic population increases, the isomer shift will decrease. However, the 4s Mulliken atomic population does not take into account the shielding effects from the 3d and the 4p electrons. In previous work [36,37], these shielding effects were considered in terms of the Slater effective nuclear charge experienced by the iron 4s electrons. As the effective nuclear charge increases, the 4s radial electronic distribution contracts, the s-electron density at the iron nucleus increases, and the isomer shift decreases.

A more accurate calculation of the effective nuclear charge experienced by the iron 4s electrons can be obtained by using the method of Clementi and Raimondi [38]. In this method, Clementi and Raimondi used self-consistent field wave functions to obtain the shielding experienced by an electron. Both the Slater and the Clementi and Raimondi effective nuclear charges, Z_{eff}, experienced by the iron 4s electrons were calculated from the iron Mulliken atomic populations [38,39], and are given in Table 2. A better representation of the s-electron density at the iron nucleus may be obtained by considering both the iron 4s Mulliken atomic population and the effective nuclear charge they experience. Figure 6, which includes clusters in this and related work [24,31,36,37,40,41], shows the correlation between the sum of the iron 4s population and the Clementi and Raimondi effective nuclear charge and the isomer shift. When all the data is considered, this plot has a slope of −0.88 mm/s per electron, an intercept of 4.47 mm/s, and a correlation of 0.86.

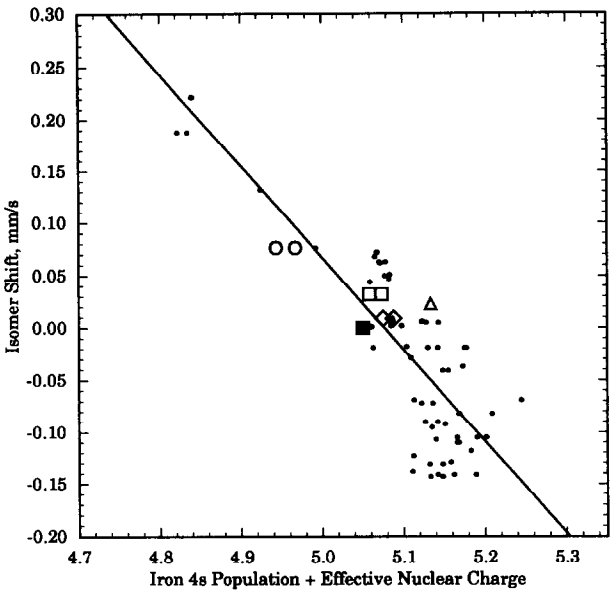

Fig. 6. The iron-57 isomer shift versus the sum of the iron 4s Mulliken atomic population and the Clementi and Raimondi effective nuclear charge experienced by the iron 4s electrons for Fe(1) (■), and Fe(2,3) (□), in $H_2Fe_3S(CO)_9$ (I), Fe(1,2) (◇) in $HFe_2CoS(CO)_9$ (II), Fe(1) (△), in $FeCo_2S(CO)_9$ (III), and Fe(1,2) (○) in $Fe_2S_2(CO)_6$ (V). The smaller points represent values obtained for a variety of related clusters, see text for references.

Figure 6 shows that, for these iron-cobalt clusters, the Mössbauer effect isomer shift is more sensitive to the iron s-electron density at the nucleus, than is the iron 4s orbital population or the Clementi and Raimondi effective nuclear charge which they experience. Within the ± 0.005 mm/s isomer shift accuracy, Fig. 6 and Table 1 reveal there are two different s-electron environments at the iron nuclei in these iron-cobalt clusters. The isomer shifts of Fe(1) in **I** and of Fe(1,2) in **II**, 0.000(5) and 0. 009(5) mm/s, respectively, are similar. This indicates that the s-electron density at the iron nucleus is similar whether its near-neighbor environment is two iron-hydrogen groups, as for Fe(1) in **I**, or is one iron-hydrogen group and one cobalt atom, as for Fe(1,2) in **II**. Also the isomer shifts for Fe(2,3) in **I** and for Fe(1) in **III**, 0.032(5) and 0.023(5) mm/s, respectively, are similar. This indicates that the s-electron density at the iron nucleus is similar whether its near-neighbor environment is two iron-hydrogen groups, as for Fe(2,3) in **I**, or is two cobalt atoms, as for Fe(1) in **III**. The effect of an iron-hydrogen group or a cobalt atom, which are isoelectronic, on the s-electron density at an iron nucleus is similar. In contrast, the coordination of the two bridging sulfur atoms in **V** both reduces the iron s-electron density and effective nuclear charge, and increases the isomer shift.

TABLE 4. A comparison of the observed and calculated quadrupole splittings [a]

Cluster	Site	Obs.	Calc. total			Calc. valence					Calc. lattice			
		ΔE_Q	ΔE_Q	V_{zz}	η	ΔE_Q	V_{zz}	η	$\langle r^{-3}\rangle_{3d}$	%	ΔE_Q	V_{zz}	η	%
$H_2Fe_3S(CO_9)$ (I)	Fe(1)	0.563	−1.51	−0.71	0.38	−1.50	−0.71	0.38	31.1	99	−0.01	−0.01	0.33	1
	Fe(2)	1.046	1.44	0.68	0.26	1.44	0.68	0.28	31.1	99	−0.01	−0.01	0.93	1
	Fe(3)	1.046	1.44	0.63	0.76	1.44	0.63	0.77	31.2	99	0.01	0.01	0.76	1
$HFe_2CoS(CO)_9$ (II)	Fe(1)	0.689	0.86	0.37	0.82	0.85	0.37	0.83	31.2	99	−0.02	−0.01	0.81	1
	Fe(2)	0.689	0.91	0.39	0.87	0.91	0.39	0.86	31.2	99	0.01	0.01	0.92	1
	Co	–	–	−0.32	0.46	–	−0.32	0.49	32.0	–	–	−0.01	0.41	–
$FeCo_2S(CO)_9$ (III)	Fe	0.780	0.65	0.28	0.90	0.65	0.28	0.86	31.3	99	−0.02	−0.01	0.63	1
	Co(1)	–	–	−0.49	0.52	–	−0.49	0.52	32.0	–	–	−0.01	0.44	–
	Co(2)	–	–	0.36	0.99	–	−0.36	0.99	32.0	–	–	−0.01	0.41	–
$Fe_2S_2(CO)_6$ (V)	Fe(1)	1.109	1.27	0.58	0.54	1.27	0.58	0.54	30.9	100	0.00	0.00	0.69	0
	Fe(2)	1.109	1.27	0.57	0.70	1.28	0.57	0.70	30.8	99	−0.01	0.00	0.48	1

[a] The ΔE_Q values were obtained at 78 K and have units of mm/s. V_{zz} values have units of V/m^2 and must be multiplied by 10^{22}.

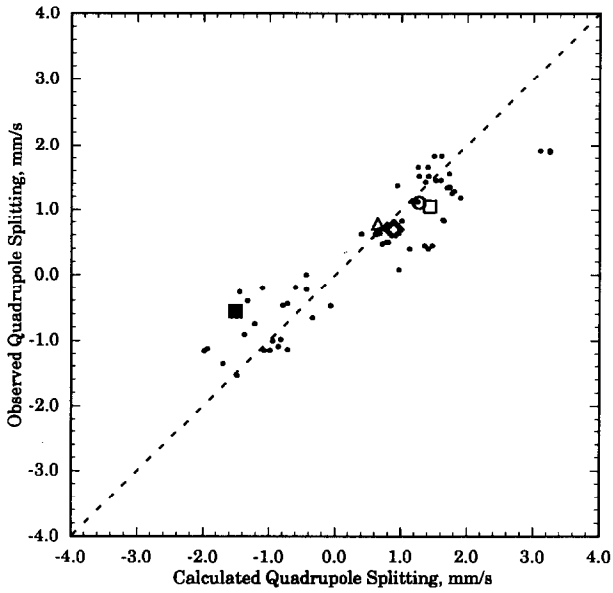

Fig. 7. The observed and calculated quadrupole interactions for Fe(1) (■), and Fe(2,3) (□), in $H_2Fe_3S(CO)_9$ (I), Fe(1,2) (◇) in $HFe_2CoS(CO)_9$ (II), Fe(1) (△) in $FeCo_2S(CO)_9$ (III), and Fe(1,2) (○) in $Fe_2S_2(CO)_6$ (V). The smaller points represent values obtained for a variety of related clusters, see text for references. The dashed line is the unit slope and *not* a fit to the data.

3.4. Mössbauer effect quadrupole interaction

The contributions to the electric field gradients, calculated from the molecular orbital wave function coefficients and the Mulliken atomic charges, are given in Table 4. In these clusters the valence contribution is the major contribution to the electric field gradient. The non-integral, nonequivalent iron 3d and 4p orbital populations, lead to the dominance of the valence over the lattice contribution to the electric field gradient.

The experimental values of ΔE_Q are compared with the calculated values in Fig. 7 which also includes data for several series [24,31,36,37,40,41] of related organoiron clusters. Because the Mössbauer effect only yields the magnitude of ΔE_Q, the sign of the calculated value of ΔE_Q was assigned to the experimental value of ΔE_Q. Figure 7 shows that the Fenske–Hall molecular orbital calculations are useful in predicting the electric field gradients in clusters.

One explanation for the disagreement between the observed and the calculated values of ΔE_Q for Fe(1) in **I** is our neglect of the Sternheimer factors, γ_∞ and R, which should be included in the calculated value of the electric field gradient. These factors take into consideration the polarization of the symmetric electronic core distribution by the non-spherical lattice and valence electronic distributions. Because the lattice contribution is small, the Sternheimer antishielding factor, γ_∞, may be neglected. However, the Sternheimer shielding factor, R, could be substantial, especially when the calculated quadrupole interaction is large. Thus the inclusion of R would decrease the calculated values of ΔE_Q in clusters **I** and **II**. Another explanation is that the structure used for cluster **I** for the molecular orbital and electric field gradient calculations is not its X-ray crystal structure but is the appropriately modified structure of cluster **III**. It has been found that small differences in the structure of a cluster will change the molecular orbital wave function coefficients obtained from the molecular orbital calculation and in turn change the results of the electric field gradient calculation by as much as fifteen percent.

The calculated values of ΔE_Q may be explained in terms of the structure chosen for these clusters. As mentioned above, the structures of clusters **I** and **II** are based upon cluster **III**. Hence, the metal, sulfur, and carbonyl ligand positions do not change in these iron-cobalt clusters. The Fe(1) site of cluster **I** has the largest calculated value of ΔE_Q, and therefore the least symmetry of these iron sites. This Fe(1) site also has the largest coordination number in these clusters. As the near-neighbor iron-hydrogen group is replaced by a cobalt atom, the coordination number of the iron site decreases, the symmetry of the iron site increases, and the calculated value of ΔE_Q decreases. The observed values of ΔE_Q show the opposite effect of the replacement of an iron-hydrogen group by a cobalt atom. The Fe(1) site of cluster **I** was observed to have the most symmetric electronic environment, despite the high coordination number. This is an indication that the positions of the hydrogens in the structures of clusters **I** and **II** may be slightly wrong. The difference between the observed and the calculated ΔE_Q values of cluster **III**, the cluster for which the known X-ray structure was used, is the smallest for these iron-cobalt clusters.

4. Conclusions

This study has shown that both Mössbauer spectroscopy and the results of Fenske–Hall molecular orbital calculations may be used to gain a better understanding of the electronic properties in these clusters. The cobalt carbonyl ligand charge is nearly constant, which leads to the nearly constant cobalt charge. The electron density donated to the iron atoms by the iron carbonyl ligands is partially delocalized onto the bridging hydrogens. When the iron and hydrogen charges are added, the sum increases as the iron carbonyl ligand charge decreases. The sulfur charge becomes more positive as the more electronegative cobalt content increases. The HOMO–LUMO gap increases as the iron content in these clusters increases.

The Mössbauer effect is very sensitive to the changes in the electronic environment of an iron nucleus. The isomer shift is best represented by the sum of the iron 4s Mulliken orbital population and the Clementi and Raimondi effective nuclear charge which they experience. The isomer shifts indicate that there are two different s-electron densities at the iron nuclei in these clusters. The s-electron density at the nuclei of Fe(1) in cluster **I** and Fe(1,2) in cluster **II** are similar. Likewise that of Fe(2,3) in cluster **I** and Fe(1) in cluster **III** are similar. The effect on the s-electron density of the iron with a near-neighbor iron-hydrogen group or cobalt atom is similar.

Acknowledgments

The authors thank Drs. L. Biolsi, G. Bertrand, A. Penico, F. Grandjean and D.E. Tharp for helpful discussions during the course of this work. The authors also thank the donors of the Petroleum Research Fund, administered by the American Chemical Society.

References and notes

1 M.L. Buhl, PhD Thesis, University of Missouri-Rolla, 1993.
2 P.T. Chesky and M.B. Hall, *Inorg. Chem., 22* (1983) 2102.
3 P.T. Chesky and M.B. Hall, *Inorg. Chem., 22* (1983) 2998.
4 A.J. Hempleman, I.A. Oxton, D.B. Powell, P. Skinner, A.J. Deeming and L. Markó, *J. Chem. Soc., Faraday Trans. II*, 77 (1981) 1669.
5 G.C. A Schuit and B.C. Gates, *AIChE Journal, 19* (1973) 417.
6 C.N. Satterfield, *Chemtech, 11* (1981) 618.
7 D.P. Burke, *Chem Week, 124* (1979) 42.
8 J.B. McKinley, in P.H. Emmett (ed.), *Catalysis Volume V*, Reinhold, New York, 1957, p. 405.
9 C.N. Satterfield, *Heterogeneous Catalysis in Practice*, McGraw-Hill, New York, 1980.
10 J.A. Cusumano, R.A. Dalla Betta and R.B. Levy, *Catalysis in Coal Conversion*, Academic Press, New York, 1978.
11 D.L. Stevenson, H.W. Chin and L.F. Dahl, *J. Am. Chem. Soc., 93* (1971) 6027.
12 C.E. Strouse and L.F. Dahl, *J. Am. Chem. Soc., 93* (1971) 6032.
13 S. Aime, L. Milone, R. Rossetti and P.L. Stanghellini, *Inorg. Chim. Acta, 25* (1977) 103–108.
14 L. Markó, *J. Organomet. Chem., 213* (1981) 271.
15 L. Markó, J. Takács, S. Papp and B. Markó-Monostory, *Inorg. Chim. Acta, 45* (1980) L189.
16 S. Khattab, L. Markó, G. Bor and B. Markó, *J. Organomet. Chem., 1* (1964) 373.
17 B.E. Bogan, Jr., D. A. Lesch and T.B. Rauchfuss, *J. Organomet. Chem., 250* (1983) 429.
18 R.F. Fenske, *Pure and Applied. Chem., 27* (1971) 61.
19 M.B. Hall and R.F. Fenske, *Inorg. Chem., 11* (1972) 768.
20 F. Herman and S. Skillman, *Atomic Structure Calculations*, Prentice-Hall, Englewood Cliffs, NJ, 1963.
21 B.E. Bursten and R.F. Fenske, *J. Chem. Phys., 67* (1977) 3138.
22 B.E. Bursten, R.J. Jensen and R.F. Fenske, *J. Chem. Phys., 68* (1978) 3320.
23 See instructions provided with the Fenske–Hall code.
24 M.L. Buhl, G.J. Long and J.F. O'Brien, *Organometallics, 12* (1993) 283.
25 R. Bau, R.G. Teller, S.W. Kirtley and T.F. Koetzle, *Acc. Chem. Res., 12* (1979) 176.
26 A. Trautwein, F.E. Harris and I. Dezsi, *Theoret. Chim. Acta (Berl.), 35* (1974) 231.
27 J.L.K.F. De Vries, C.P. Keijzers and E. De Boer, *Inorg. Chem., 11* (1972) 1343.
28 M. Weissbluth and J.E. Maling, *J. Chem. Phys., 47* (1967) 4166.
29 Markó *et al.* [14,15] reported their observed hyperfine parameters at 78 K relative to platinum. The following isomer shift values have been changed to correspond to α-iron foil by adding 0.349 mm/s to the isomer shift. For $H_2Fe_3S(CO)_9$ (**I**), they observed isomer shifts of -0.141 and -0.051 mm/s and quadrupole splittings of 0.76 and 0.95 mm/s for Fe(1) and Fe(2,3), respectively. For $HFe_2CoS(CO)_9$ (**II**), they observed an isomer shift of -0.091 mm/s and a quadrupole splitting of 0.67 mm/s.
30 J.E. Huheey, *Inorganic Chemistry: Principles of Structure and Reactivity, 3rd Edition*, Harper and Row, New York, 1983, pp. 141–149.
31 M.L. Buhl, G.J. Long and J.F. O'Brien, *Organometallics, 12* (1993) 1902.
32 E.L. Muetterties, T.N. Rhodin, E. Band, C.F. Brucker and W.R. Pretzer, *Chem. Rev., 79* (1979) 91.
33 G.A. Somorjai; *Science, 227* (1985) 902.
34 J.E. Huheey, *Inorganic Chemistry: Principles of Structure and Reactivity, 3rd Edition*, Harper and Row, New York, 1983, p. 592.
35 The differences in the results of the molecular orbital calculations are probably due both to differences in the basis sets used and in the molecular geometry chosen for the clusters. Chesky and Hall [3] used the Clementi and Richardson basis functions and the molecular geometry of the iron-cobalt clusters was based upon that of $Co_3S(CO)_9$. We chose to use the Herman and Skillman basis functions so that our results could be compared with results for other series of clusters [24,31,36,37,40,41]. We based the molecular geometry of the iron-cobalt clusters on the crystal structure of $FeCo_2S(CO)_9$ (**III**).
36 G.J. Long and J.F. O'Brien, *Hyperfine Interactions, 40* (1988) 101.
37 C.G. Benson, G.J. Long, J.S. Bradley, J.W. Kolis and D.F. Shriver, *J. Am. Chem. Soc., 108* (1986) 1898.
38 J.E. Huheey, *Inorganic Chemistry: Principles of Structure and Reactivity, 3rd Edition*, Harper and Row, New York, 1983, pp. 37–38.
39 J.C. Slater, *Phys. Rev., 36* (1930) 57.
40 C.G. Benson, G.J. Long, J.W. Kolis and D.F. Shriver, *J. Am. Chem. Soc., 107* (1985) 5297.
41 M.L. Buhl, G.J. Long and G. Doyle, *J. Organomet. Chem., 461* (1993) 187.